European Radiology (2019) 29:5731–5741
https://doi.org/10.1007/s00330-019-06154-3

HEPATOBILIARY-PANCREAS

Non-branched microcysts of the pancreas on MR imaging of patients with pancreatic tumors who had pancreatectomy may predict the presence of pancreatic intraepithelial neoplasia (PanIN): a preliminary study

Marie-Pierre Vullierme[1] · Lina Menassa[2] · Anne Couvelard[3] · Vinciane Rebours[4] · Frédérique Maire[4] · Tony Ibrahim[5] · Jerome Cros[3] · Philippe Ruszniewski[4] · Alain Sauvanet[6] · Philippe Levy[4] · Philippe Soyer[7] · Valerie Vilgrain[1]

Received: 20 December 2018 / Revised: 14 February 2019 / Accepted: 11 March 2019 / Published online: 10 April 2019

Abstract

Purpose To evaluate whether pancreatic parenchymal abnormalities on magnetic resonance imaging (MRI) are associated with pancreatic intraepithelial neoplasia (PanIN) on histology.

Materials and methods Retrospective study approved by institutional review board. One hundred patients (48 men, 52 women; mean age, 53.2 ± 16.29 [SD]) underwent MRI before pancreatectomy for pancreatic tumors analyzed by two independent observers blinded to histopathological results for the presence of non-communicating microcysts and pancreatic atrophy (global or focal) beside tumors. MRI findings were compared to histopathological findings of resected specimens. Interobserver agreement was calculated. The association between parenchymal abnormalities and presence of PanIN was assessed by uni- and multivariate analyses.

Results PanIN was present in 65/100 patients (65%). The presence of microcysts on MRI had a sensitivity of 52.3% (34/65 [95%CI, 51.92–52.70%]), a specificity of 77.1% (27/35 [95%CI, 76.70–77.59]), and accuracy of 61% (61/100 95%CI [50.7–70.6]) for the diagnosis of PanIN while global atrophy had a sensitivity of 24.6% (16/6 [95%CI, 24.28–24.95]) and a specificity of 97.1% (34/35 [95%CI, 96.97–97.32%]). In multivariate analysis, the presence of microcysts (OR, 3.37 [95%CI, 1.3–8.76]) ($p = 0.0127$) and global atrophy (OR, 9.79 [95%CI, 1.21–79.129]) ($p = 0.0324$) were identified as independent predictors of the presence of PanIN. The combination of these two findings was observed in 10/65 PanIN patients and not in patients without PanIN ($p = 0.013$ with an OR of infinity [95%CI, 1.3–infinity]) and was not discriminant for PanIN-3 and lower grade ($p = 0.22$). Interobserver agreement for the presence of microcysts was excellent (kappa = 0.92), and for the presence of global atrophy, it was good (kappa = 0.73).

Conclusion The presence of non-communicating microcysts on pre-operative MRI can be a significant predictor of PanIN in patients with pancreatic tumors.

Key Points

- *In patients with pancreatic tumors who had partial pancreatectomy, MR non-communicating pancreatic microcysts have a 52.3% sensitivity, a 77.1% specificity, and a 61% accuracy for the presence of PanIN with univariate and with an odds ratio of 3.37 with multivariate analyses.*
- *The association of global atrophy and non-communicating microcysts increases the predictive risk of PanIN.*

Keywords Carcinoma, pancreatic ductal · Magnetic resonance imaging (MRI) · Cysts · Pancreatectomy

✉ Marie-Pierre Vullierme
marie-pierre.vullierme@aphp.fr

[1] Paris Diderot University, Sorbonne Paris Cité, INSERM U1149 CRB3, Paris, France

[2] Imaging Department, Hotel-Dieu de France Hospital, Beirut, Lebanon

[3] Department of Pathology, Beaujon University Hospital, Clichy, France

[4] Department of Pancreatology, Beaujon University Hospital, Clichy, France

[5] Oncology Department, Clinical Research Units, Clinical Biostatistical Research Units, Saint Joseph University, Beirut, Lebanon

[6] Department of Hepato Pancreato Biliary Surgery, Beaujon University Hospital, Clichy, France

[7] Department of Radiology, Cochin University Hospital, Paris, France

Abbreviations

BD-IPMN	Branch duct IPMN
IPMN	Intraductal papillary mucinous neoplasm
Microcysts	Pancreas, non-communicating micro cysts
MRCP	MR imaging with MR cholangiopancreatography
MRI	Magnetic resonance imaging
NET	Neuroendocrine tumors
P-NET	Pancreas NET
Pancreatic carcinoma	Pancreatic ductal carcinoma
PanIN	Pancreatic intraepithelial neoplasia
SPPT	Solid and pseudo papillary tumors

Introduction

Pancreatic intraepithelial neoplasia (PanIN) is a microscopic papillary or flat epithelial neoplasm that develops in the pancreatic acinus either in the absence of acinus dilatation or with a dilatation < 5 mm. Based on the degree of cellular and nuclear atypia, PanIN progresses from PanIN-1 (low-grade dysplasia), characterized by hyperplastic ductal atypia, to PanIN-2 (moderate dysplasia) and PanIN-3 (carcinoma in situ or high-grade dysplasia) [1–3].

Although PanIN-1 is observed in up to 40% of adults in the absence of invasive pancreatic carcinoma [4, 5], PanIN-2 is often described in association with pancreas abnormalities and PanIN-3 is always associated with pancreas anomalies [6]. Recently, early-stage PanIN-2 lesions have been shown to contain many somatic gene alterations involved in the development of pancreatic carcinoma [6, 7]. PanIN lesions are more frequent in patients with intraductal papillary mucinous neoplasm (IPMN) and PanIN-3 lesions are seen in 11% and 26% of patients with benign and malignant IPMN, respectively [8].

PanIN is a microscopic lesion that is theoretically impossible to visualize macroscopically. However, cystic changes (< 5 mm by definition) are part of the spectrum of PanIN lesions on pathology and may be detected by imaging studies [1, 3, 4]. Actually, we decided to work on that topic having observed some of our patients with small non-communicating microcysts on MRI whose pathologic specimen of total pancreatectomy showed PanIN-3 (Fig. 1).

PanIN lesions may also be associated with focal or extended pancreatic fibrosis, and a consensus conference has stated that chronic pancreatitis may be associated with atrophy [1, 7–10]. Therefore, we hypothesized that both mild pancreatic acinar dilatation appearing as microcysts or the accompanying or resulting fibrosis appearing as foci of abnormal signal and/or pancreatic atrophy could be visible on magnetic resonance imaging (MR imaging) [9–11].

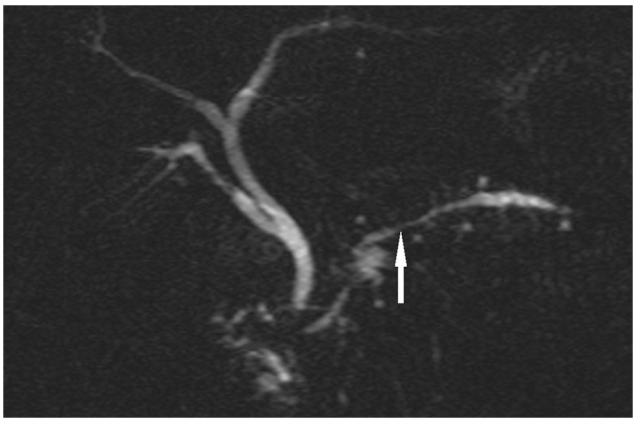

Fig. 1 Index case suggesting us to work on a possible association between MR findings and PanIN. A 53-year-old man who underwent Whipple procedure for pancreas adenocarcinoma. Abundant PanIN-3 was present. A preventive, secondary total pancreatectomy was discussed, but a pancreas adenocarcinoma developed in the tail of the pancreas 8 months following Whipple procedure. 2D-MRCP images in the coronal plane that are repeated in different angles show multiple non-communicating microcysts of the all pancreatic parenchyma. The tumor appears as a round ill-defined hypersignal. Mild stricture of the main pancreatic duct related to the tumor (arrow)

A successful screening protocol for the detection of pancreatic cancer should identify patients at risk of developing pancreatic cancer such as those with PanIN-2 and PanIN-3 [12–15]. At the same time, genomic sequencing has shown that pancreatic cancer progresses from initial to metastatic stages over a 15-year period, suggesting that early detection could play a major role in this disease [7, 15, 16]. As well, progression from PanIN-1 to PanIN-3 and from PanIN-3 to cancer seems to be slow with a simulation virtual model [17]. Until now, no biological or imaging procedures have been shown to be effective in the detection of premalignant lesions especially in high-risk patients [13, 14, 18] (that is, with inherited predisposition such as Peutz-Jeghers syndrome, hereditary pancreatitis, familial atypical mole multiple melanoma, familial BRCA2) [14], or familial pancreatic cancer (6.4 to 32-fold) [14]. These patients are included in the screening process, mainly by MR imaging, throughout the world.

Several studies have reported an increased risk of pancreatic cancer in patients with pancreatic cysts, particularly when multiple, whatever the etiology and size [1, 10, 14, 19, 20]. In some cases, and especially in high-risk patients, MR imaging with MR cholangiopancreatography (MRCP) and diffusion-weighted MR sequences help identify very small round cysts without pattern of communication with the pancreatic ducts [20–24]. The nature of these very small cysts is still unclear (Fig. 1).

Until now, endoscopic ultrasound has been the single validated imaging tool to identify indirect findings (microcysts or foci of fibrosis) associated with PanIN [8, 25]. However, the value of MR imaging has not yet been studied for this purpose.

The goal of this study was to retrospectively evaluate whether pancreatic parenchymal abnormalities seen on MR imaging and MRCP including non-communicating microcysts are associated with the presence of PanIN on surgical specimens.

Material and methods

Patients

This study was approved by our Institutional Review Board and the requirement for informed consent was waived.

A total of 1202 patients underwent pancreatectomy in our institution from August 2007 to October 2014. The selection of our patient population had two goals: first, to have a close imaging–pathological correlation between the resected tumor and the adjacent pancreatic parenchyma and second, to avoid a selection bias. Exploring the association of microcysts and PanIN in an "as normal pancreas as possible" was our way for this preliminary study. We have chosen patients with benign pancreatic tumors and parenchyma supposed to be as normal as possible at pathology, taking into account the literature concerning pathological series of BD-IPMN, P-NET, and SPPT. A flow chart is presented in Fig. 2.

The inclusion criteria were as follows: (i) non-IPMN patients with a thin main pancreatic duct (MPD < 4 mm in the head and < 3 mm in the body tail of the pancreas) or BD-IPMN patients with MPD not larger than 6 mm (the 6-mm cut-off concerned exclusively doubtful mixed-type IPMN, requiring surgery) [26]; (ii) the presence of pancreatic parenchyma on the surgical specimen; and (iii) patients with a MR imaging examination of the pancreas according to our acquisition protocols, to limit the bias of the morphological analysis.

The following patients were excluded from the study: (i) Patients with a markedly enlarged (> 6 mm) MPD or with more than three visible thin branch ducts due to underlying obstructive disease were excluded because obstructive chronic pancreatitis branch duct enlargement can prevent visualization of the presence of microcysts. MPD enlargement was present in 181 patients with IPMN and 160 patients with MPD dilatation upstream from the resected tumor (i.e., 111 with neuroendocrine tumors (NET), 47 with mucinous cystadenoma or cystadenocarcinomas, and 2 with solid and pseudo papillary tumors (SPPT)). (ii) One hundred fifty patients with tumor enucleation were excluded, i.e., 70 NET, 35 branch duct IPMN, 17 SPPT, 14 serous cystadenomas, and 14 mucinous cystadenomas. (iii) One hundred one patients with unsatisfactory MR imaging results (movement artifacts, lack of MRCP, no injection of gadolinium chelates) were excluded, i.e., 37 patients with branch duct IPMN, 50 with NET, and 14 with SPPT.

Patients with a high predicted rate of high-grade PanIN were also excluded, such as pancreatic carcinoma (510 patients resected for pancreatic carcinoma were excluded) to avoid an inclusion bias with an oversized rate of PanIN-3, knowing that PanIN-3 is known to be associated with pancreas adenocarcinoma.

The mean interval between MR imaging and surgery was 118 days ± 102 (SD) (range, 1–290 days). All indications for surgical resection were discussed during a multidisciplinary team meeting. Briefly, indications for resection of IPMN included worrisome features or high-risk stigmata of malignancy according to the international conference of experts [26], in particular cysts > 3 cm (9 patients), doubtful mixed-type IPMN on endoscopic ultrasound and MR imaging results (17 and 5 patients with the main pancreatic duct measuring 6 mm and 5 mm, respectively), and mural nodules (9 patients). Patients with NET or SPPT underwent resection due to the risk of malignancy.

MR imaging protocol

All MR imaging examinations were performed using consecutively a 1.5-T and 3-T device (Intera®, Ingenia®; Philips Healthcare) (Table 1). The MR imaging protocol included axial fat-suppressed T2-weighted spectral presaturation with inversion recovery (SPIR) sequences, axial and coronal T2-weighted single-shot half-Fourier (SSH) sequences, and axial T1-weighted gradient echo sequences. Axial three-dimensional (3D) T1-weighted ultra-fast gradient echo (THRIVE®, mDixon) sequences were obtained after intravenous administration of 0.1 mmoL/kg of body weight of gadoterate meglumine using a power injector at a flow rate of 2 mL/s (at 30, 70, and 120 s).

MRCP images were obtained with coronal and sagittal 2D heavily T2-weighted radiated thick slices (25 mm) and coronal 3D T2-weighted thin slices. The same protocol has been performed since 2007 using the same equipment (1.5 T then 3 T since November 2012) with minimal changes.

Image analysis and imaging criteria

MR imaging examinations were reviewed on a picture archiving and communication system (PACS) workstation (Directview®, 11.3 version, Carestream Health Inc) by two abdominal radiologists (L.M. and M-P.V. with 15 and 25 years of experience in MR imaging of the pancreas). The two radiologists evaluated images independently and were blinded to the results of the histopathological examinations.

Several MR imaging findings were evaluated using a standardized data collection form including the presence of non-communicating microcysts, atrophy of the pancreatic parenchyma and focal, small, pancreatic obstructive lobular lesions. In case of disagreement between the two observers, a consensus was reached and these results were used for further statistical analysis.

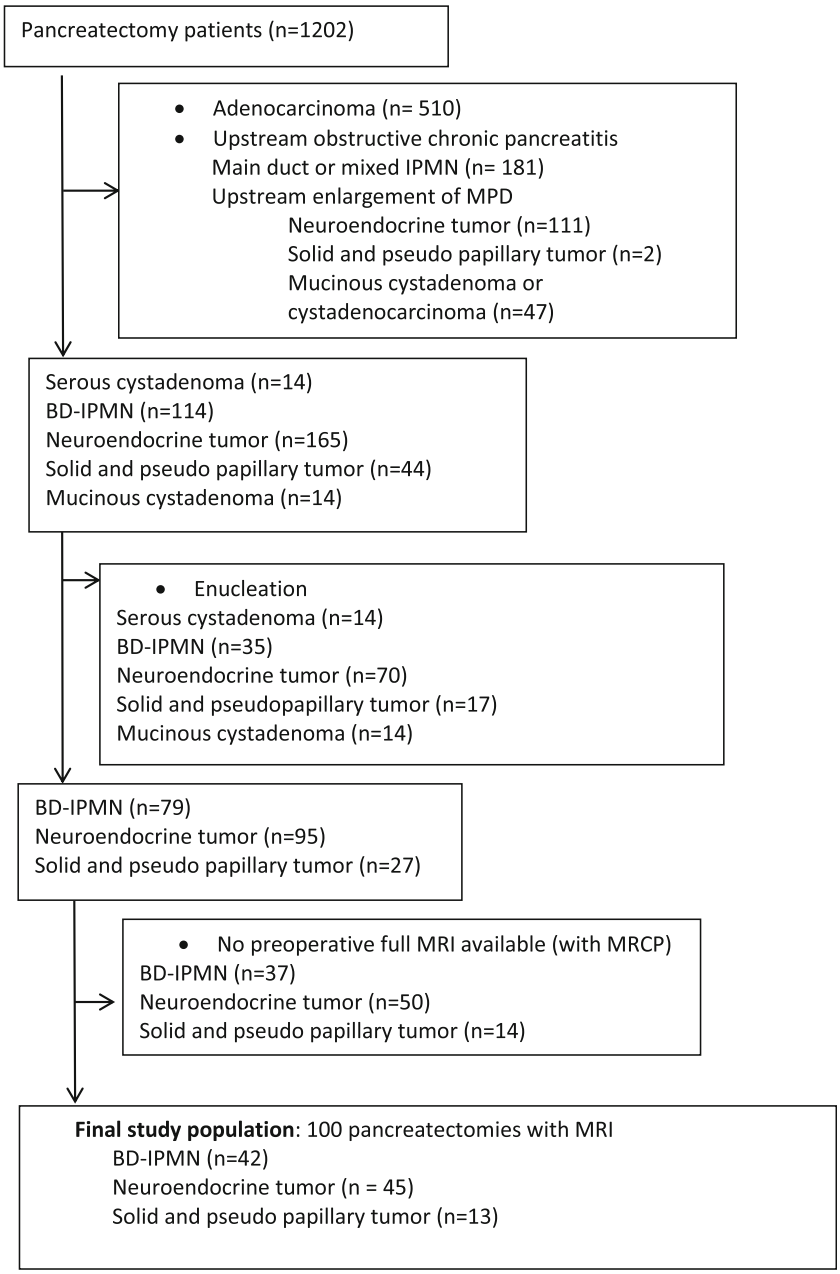

Fig. 2 Flow chart diagram. IPMN indicates intraductal papillary mucinous neoplasm; BD-IPMN, branch duct intraductal papillary mucinous neoplasm; MRI, magnetic resonance imaging; MPD, main pancreatic duct

A non-communicating microcyst was defined as a round cyst no more than 5 mm in diameter, with no ducts surrounding the cyst, and no tubular pattern communicating with downstream ducts. The size of ≤ 5 mm was based on the histopathological definition of PanIN [2–4]. If a non-branched microcyst was identified, it was analyzed for location (head, body, or tail), its largest diameter was measured, and cysts were counted.

Pancreatic atrophy was considered to be present when the largest anteroposterior thickness of the pancreas was < 2 cm [12]. It was categorized as global when it involved more than one-third of the pancreatic parenchyma or focal when it involved less than one-third [27, 28].

Stigmata of focal obstructive lobular lesions was considered to be present on MR imaging when the pancreatic parenchyma had small (< 1 cm) foci of decreased signal intensity compared with the liver on fat-suppressed T1-weighted MR images that were hyperintense on portal venous or delayed phase MR images compared with the adjacent pancreas [4, 9, 27, 28].

Standard of reference

All pancreatic surgical specimens were sliced using the bread loaf technique for left pancreatectomies and the axial slicing technique for pancreaticoduodenectomies with 5-mm slices.

Table 1 Imaging parameters used for MR imaging and MR cholangiopancreatography (1.5 T, 3 T)

MR sequence	*N* of sections	TR/TE (ms)	Flip angle (°)	Matrix size	Voxel size (mm)	Section thickness (mm)	Nex
T2-weighted single-shot sequence	32	890/85	90	320 × 320		*5*	1
	42	*433/120*	*90*	*188 × 216*	*1.60 × 1.65*	*4*	*1*
T2-weighted fast spin-echo sequence with spectral fat saturation	36	1800/90	*90*	512 × 512		4	1
	32	*571/140*	*90*	*216 × 251*	*1.30 × 1.51*	*5.50*	*1*
T1-weighted fat-suppressed spoiled gradient-recalled echo sequence	90	4.6/2.2	10	240 × 240		3	2
	111	*4/1.40*	*10*	*188 × 207*	*1.60 × 1.72*	*3.60*	*1*
Diffusion-weighted	32	4033/63	90	256 × 256		6	6
	36	*1207/55*	*90*	*132 × 97*	*3.03 × 3.11*	*4.5*	*1*
2D MRCP coronal radiated	9	8000/800	90	480 × 480		25	1
	9	*8000/688*	*90*	*300 × 238*	*0.93 × 1.18*	*25*	*1*
3D MRCP	54	5371/753	90	292 × 193	1.37 × 1.95	3	1
	54	*4924/737*	*90*	*292 × 193*	*1.20 × 1.61*	*3*	*1*

TR, repetition time; *TE*, time of excitation; *Nex*, number of excitations

Italicized entries are 3T values

All macroscopic lesions were sampled. At least one sample was taken every three slices in an apparently normal pancreas. Two experienced pathologists (A.C. and J.C.) reviewed hematoxylin-eosin slides for each surgical specimen. The specimens were carefully evaluated for the presence of ductal lesions. If dysplastic cells were found lining the ductal lesions, they were classified as PanIN and graded from 1 to 3 [1–5]. If several grades of PanIN were identified, the highest grade was kept. When a dilated duct was lined by non-dysplastic flattened ductal-like cells, this lesion was classified as a mechanical microcyst. Considering the size < 5 mm, IPMN was ruled out [5].

Statistical analyses

Quantitative data were expressed as means, SDs, and ranges. Categorical data were expressed as raw numbers, proportions, and percentages. Non-parametric continuous data, in a small group, was expressed as median with interquartile range.

We compared patients with (group 1) and without (group 2) PanIN to identify variables associated with the diagnosis of PanIN on MR imaging. Qualitative variables were compared with the chi-squared test or, when not applicable, the Fisher exact test.

The unweighted Cohen Kappa test was used to assess interobserver agreement of categorical data, with kappa values of 0.00–0.20 considered to indicate poor agreement; 0.21–0.40, fair agreement; 0.41–0.60, moderate agreement; 0.61–0.80, good agreement; 0.81–0.99, excellent agreement; and 1.00, perfect agreement [29].

The sensitivity, specificity, and accuracy of the different variables for the diagnosis of PanIN were calculated with their corresponding 95% exact confidence intervals (CIs). Univariate logistic regression and multivariate analysis were performed to identify MR imaging features associated with PanIN. Odds ratios and the corresponding 95%CIs for proportions were calculated.

All statistical tests were two-tailed and $p < 0.05$ was considered to be significant. Statistical analyses were performed using the software Statistical Analysis System, SAS 9.2.

Results

Patient characteristics

There was no statistically significant difference between the two groups with and without PanIN in terms of age and gender distribution and relative proportion primary indications such as BD-IPMN, P-NET, and SPPT. The median age range was 50 (39–61.5) to 59 (49–67) years, except SPPT patients who were younger but with similar age in both groups (inherent to the epidemiology of the tumor) (Table 2).

Surgical resections were duodenopancreatectomy, $n = 46$; total pancreatectomy, $n = 4$; left pancreatectomy ± splenectomy, $n = 31$; and median pancreatectomy, $n = 19$.

Histopathological results

Microcysts < 5 mm being present at pathology were of two types, some with dysplasia permitting the diagnosis of PanIN and some without dysplasia, being also currently observed beside PanIN. These two types of microcysts were too small to be correlated each to the corresponding microcyst seen on the MRCP images (Figs. 3c and 4c).

The histopathological analysis of patients is reported in Table 2. Sixty-five (65/100; 65%) patients had PanIN; 28 (28/65; 43%) had PanIN-1, 31 (31/65; 48%) had PanIN-2; and 6 (6/65; 9%) had PanIN-3. PanIN was present in 32/42

Table 2 Demographic and histopathological findings in 100 patients

$n = 100$	No PanIN ($n = 35$)		PanIN ($n = 65$) PanIN-1 (28), PanIN-2 (31), PanIN-3 (6)	
Gender (M/W)	(12/23)		(30/35) PanIN-1 (11/17), PanIN-2 (14/17), PanIN-3 (5/1)	
Age (years)	*50 [39–61.5]*		*59 [49–67]*	
BD-IPMN ($n = 42$)	*60.5 [54.75–66.25]*	$n = 10$ (24%)	*62.5 [51.75–69.5]*	$n = 32$ (76%) PanIN-1 ($n = 17$; 53%) PanIN-2 ($n = 9$; 28%) PanIN-3 ($n = 6$; 19%)
P-NET ($n = 45$)	*55 [46–63.5]*	$n = 16$ (36%)	*58 [50–63]*	$n = 29$ (64%) PanIN-1 ($n = 8$; 28%) PanIN-2 ($n = 21$; 72%)
SPPT ($n = 13$)	*32 [24–40]*	$n = 9$ (69%)	*31 [28.5–33.5]*	$n = 4$ (31%) PanIN-1 ($n = 3$; 75%) PanIN-2 ($n = 1$; 25%)

Numbers *in italic* are the median age with [interquartile range] of each population

No PanIN, patients without pancreatic intraepithelial neoplasia; *PanIN*, patients with pancreatic intraepithelial neoplasia; *BD-IPMN*, branch duct intraductal pancreas mucinous neoplasia; *PNET*, pancreatic neuroendocrine tumor; *SPPT*, solid and pseudo papillary tumor

patients with BD-IPMN (76%), 29/45 patients with P-NET (64%), and 4/13 patients with SPPT (31%). PanIN was as frequent with IPMN as with P-NET ($p = 0.25$).

The tumor results of patients with BD-IPMN, P-NET, and SPPT corresponded to usual findings.

MR imaging results

Non-communicating microcysts were visible on MR imaging in 42/100 patients (42%) (Figs. 3 and 4) with a total of 194 microcysts (mean, 4.5 ± 3.09 [SD] per patient [1–12]). The number and size of the non-communicating microcysts identified on MR imaging were not different in patients with and without PanIN.

Results of the combinations of imaging features are shown in Tables 3, 4, and 5.

Correlation between PanIN and MR imaging findings

Non-communicating microcysts seen on MR imaging were present in 34/65 patients with PanIN (52%) and in 8/35 without (23%) ($p = 0.0044$; OR = 3.7; 95%CI, 1.5–9.4) (Figs. 3 and 4) (Table 3). Therefore, the presence of non-communicating microcysts on MR imaging had a sensitivity of 52.3%, a specificity of 77.1%, a NPV of 46.6%, a PPV of 81%, and an accuracy of 61% for the diagnosis of PanIN (Table 5). Non-communicating microcysts were present in 14 (14/28; 50%) patients with PanIN-1, 15 patients (15/31; 48%) with PanIN-2, and 5 patients (5/6; 83%) with PanIN-3.

Eighteen of the 42 patients with microcysts on MR imaging had branch duct IPMN, 1 without PanIN, and 17 with PanIN (17/18, 94%). In 42 patients with branch duct IPMN, 10 had no PanIN (10/42, 24%) and 32 had PanIN (32/42, 76%). In patients with BD-IPMN, the presence of microcysts was associated with the presence of PanIN ($p = 0.026$).

As SPPT are developed in young patients where incidence of PanIN is known to be significantly less, we have calculated the diagnostic performance without SPPT patients. Sensitivity, specificity, and negative and positive predictive values for the diagnosis of PanIN were 57%, 77%, 43%, and 85%, respectively.

Four of the eight false-positive patients had only one microcyst on MR imaging (the others had 2, 5, 6, and 6 cysts). With > 1 cyst as the criterion, the sensitivity, specificity, and negative and positive predictive values for the diagnosis of PanIN were 52%, 89%, 50%, and 80%, respectively, with a $p < 0.001$; OR, 8.5 (95%CI, 3.9–17). With > 2 cysts, the sensitivity, specificity, and negative and positive predictive values for the diagnosis of PanIN were 42%, 91%, 47%, and 90%, respectively, with a $p < 0.001$; OR, 7.7 (95%CI, 2.1–27.9).

Global atrophy of the pancreatic parenchyma was more frequent in patients with PanIN (16/65; 25%) (Table 3) (including PanIN-1 (7/16, 44%), PanIN-2 (6/16, 38%), and PanIN-3 (3/16, 18%)) than in those without (1/35; 2.8%) ($p = 0.005$). There were very few cases of focal atrophy of the pancreatic parenchyma (3/100) and this was not different between the two groups of patients. Thus, global pancreatic atrophy had a sensitivity of 25% and a specificity of 97% for the diagnosis of PanIN (Table 5).

Hypointense T1-weighted images were identified in 12/65 patients with PanIN (18.5%) and 3/35 patients without (8.6%) ($p = 0.186$, ns). Pancreatic areas of portal or delayed enhancement were not statistically different between PanIN and non-PanIN patients.

There was no significant difference for the presence of microcysts or for the diameter of the main pancreatic duct

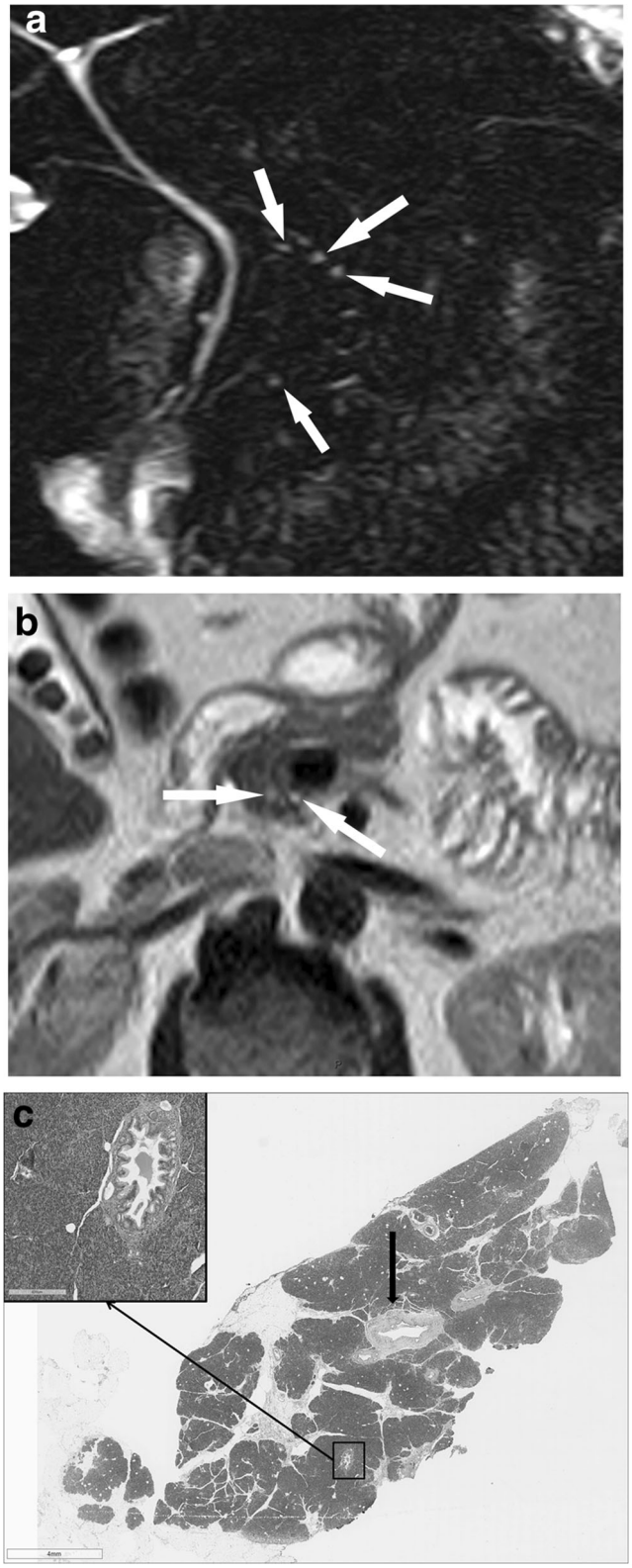

◀**Fig. 3** A 59-year-old man who underwent a Whipple procedure for a neuroendocrine tumor of the pancreatic head. PanIN-2 was identified on the histopathological analysis of resected specimen. No BD-IPMN and no chronic pancreatitis were present. **a** 2D-MRCP images in the coronal plane that are repeated in different angles show 4 non-communicating microcysts (arrows) of the pancreatic head. The main pancreatic duct is normal. **b** Axial T2-weighted SSFSE MR image shows 3 non-communicating microcysts (arrows) of the cranial and posterior part of the pancreatic head. **c** Pancreas sample (Hematoxylin Eosin Safran stain (× 10 magnification)) with PanIN-2. The arrow indicates the Wirsung duct that appears normal. The square, magnified at × 100 in the upper-left corner isolates an enlarged branch duct with PanIN-2 lesion

(assessed on MRCP) in patients with PanIN and in those without (mean diameter 3.55 to 3.58 mm in each population).

Univariate and multivariate analyses showed that non-communicating microcysts and global atrophy were the most discriminating findings to differentiate patients with and without PanIN (Table 4). The association of global atrophy and microcysts was discriminating. If both abnormalities were associated, the presence of PanIN was highly probable with a sensitivity of 15% (10/65), a specificity of 100% (0/35), a PPV of 100%, and a NPV of 39.9%.

Except for a higher rate of microcysts in patients with PanIN-3 (5/6; 83%), no other significant MR patterns were found for the different grades of PanIN.

Interobserver agreement

Interobserver agreement was excellent for the presence of non-communicating microcysts on MR imaging, good for focal atrophy, and moderate for global atrophy and hypointensity on T1-weighted images and their enhancement. Detailed Kappa values are presented in Table 3.

Discussion

This study shows that the presence of non-communicating microcysts of the pancreas on MR imaging could be associated with the presence of histologically diagnosed PanIN on surgical specimens. MRI showed no microcysts in 58% of our study population and 73% of patients with no PanIN had no microcysts seen on MR.

Microcysts were identified microscopically in all our patients with microcysts on MR imaging and PanIN on pathology, suggesting these cysts may be strongly hyperintense on T2- and MRCP images. In fact, they are filled with pancreatic juice. Although communication between PanIN microcysts and pancreatic ducts has frequently been identified in pathological studies, this communication is probably too small to be visible on MR imaging [1, 3]. While there was a significant correlation between the presence of microcysts on MR imaging and PanIN on pathology, false-positive and false-negative cases were observed. Small cysts (3–5 mm) identified on imaging may not be found in the final pathological examination either because they are contained in thick tissue "slices" that

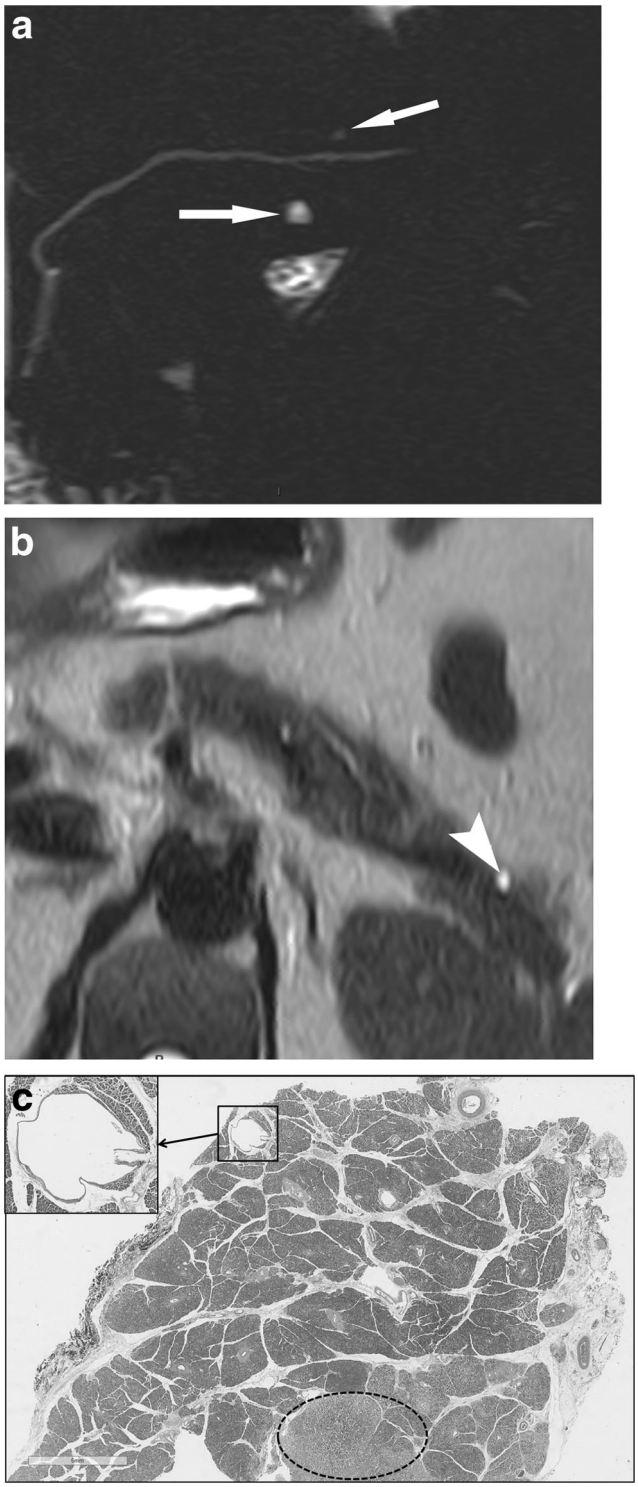

◀**Fig. 4** A 63-year-old-woman who underwent a left pancreatectomy for a neuroendocrine tumor of the pancreatic tail. PanIN-1 was identified at histopathological analysis of the resected specimen. No BD-IPMN and no chronic pancreatitis were present. The parenchyma was diffusely atrophied. **a** 2D-MRCP images in the coronal plane that are repeated in different angles show two non-communicating microcysts (arrows) of the pancreatic body. The main pancreatic duct is normal. **b** Axial T2-weighted SSFSE MR image shows one additional microcyst in the tail of the pancreas (arrowhead). Body and tail of the pancreas are small and globally atrophied. **c** Pancreas sample (Hematoxylin Eosin Safran stain (× 10 magnification)) with resected G2 TNE (dotted circle) and PanIN (not shown). Microcyst secondary to focal duct obstruction, 2 mm (square and magnification), adjacent to the resected tumor

are larger than the cyst or because they are mistaken for retention cysts during macroscopic examination and not sampled.

All grades of PanIN are not associated with the same risk of developing pancreatic carcinoma and the risk is higher in PanIN-3 [6, 30]. Microcysts on MR imaging were present in 83% of patients with PanIN-3 and we did not identify different MR patterns according to the different pathological grades. Our results are similar to those by Matsuda et al, which showed cystic changes in 71% of the pancreas with PanIN-3 [1].

Although a reliable diagnosis of PanIN was only possible on histopathology in the past, recent studies have reported that endoscopic ultrasound shows pancreatic abnormalities suggesting PanIN [8, 25, 31]. PanIN lesions were observed in 78% of cases in a series of 40 patients who underwent resection for IPMN, and endoscopic ultrasonography changes (microcysts and/or hyperechoic foci) corresponded to PanIN lesions in 83% of cases. Like our results with MR imaging, endoscopic ultrasonography could not differentiate the three grades of PanIN [8].

It is interesting to note that patients with pancreatic cysts have a significantly higher overall risk of pancreatic carcinoma, although most studies lack radiopathological correlations [1, 20, 21, 23]. Munigala et al reported a hazard ratio of 19.64 for pancreatic carcinoma in all patients with macrocysts compared with those without [21]. In a screening program for familial pancreatic cancer, five of 125 at-risk individuals with multiple, small (2–10 mm) unicystic lesions and/or multicystic single lesions on MR imaging underwent surgical resection, and all had PanIN-2 and PanIN-3 lesions on histology. Four of these five patients also had branch duct IPMN, which raises the problem of a differential diagnosis [20].

In our series, global atrophy of the pancreatic parenchyma was more frequent in patients with PanIN than in those without. Focal hypointensity on T1-weighted images and their enhancement was not associated with the presence of PanIN on histology. Pathologically, PanINs produce obstructive lobular atrophy [1, 9]. PanIN-3 is accompanied by higher grade extralobular fibrosis [1]. A few reports have described endoscopic ultrasound features associated with lobular atrophy in PanIN, such as hyperechoic foci without shadowing and lobularity with honeycombing [8, 25]. It is not surprising that MR imaging is less accurate than endoscopic ultrasound in detecting these subtle features because of the lower spatial resolution of the former [20, 24].

Indeed, we excluded patients with pancreatic carcinoma because most of these patients would have had pancreatic duct dilatation and the high incidence of PanIN-3 associated with

Table 3 Comparison of MR imaging findings for categorical criteria between 65 patients with PanIN (group 1) and 35 patients without PanIN (group 2) with interobserver agreement for categorical MRI variables in 100 patients (kappa)

Variable	Group 1 (PanIN +)		Group 2 (PanIN−)		*p* value	*k* value	95%CI
	Pr	%	Pr	%			
Microcysts	34/65	52.3	8/35	22.9	0.0044	0.92	[0.83–1.00]
Global atrophy	16/65	24.6	1/35	2.8	0.005*	0.73	[0.53–0.94]
Focal atrophy	1/65	1.5	2/35	5.7	0.34*	0.82	[0.58–1]
T1 hypointense foci	12/65	18.5	3/35	8.6	0.186*	0.60	[0.38–0.81]
Size mean (std.dev.)	13 (7)		12 (13)		0.35		
Enhancement (portal or late)	10/12	83	3/3	100	0.58	0.55	[0.39–0.80]
Global atrophy and microcysts	10/65	15.4	0/35	0	0.0134*		
Global atrophy or microcysts	30/65	46.2	9/35	25.7	0.007		
No atrophy nor microcysts	25/65	38.5	26/35	74.3	0.0006		

Pr, proportion; %, percentage. Significance was searched for using the χ^2 test or *Fisher exact test. The unweighted Cohen Kappa test was used. The rating was as follows: κ values of 0.00–0.20 were considered to indicate poor agreement; κ values of 0.21–0.40, fair agreement; κ values of 0.41–0.60, moderate agreement; κ values of 0.61–0.80, good agreement; κ values of 0.81–0.99, excellent agreement; and κ value of 1.00, perfect agreement [29]. 95%CI indicates confidence interval

pancreatic carcinoma would have created a selection bias. Our population included patients with IPMN, neuroendocrine tumors, and SPPT. Interestingly, patients with SPPT had a significantly lower percentage of PanIN on histology, which might be related to the younger age of these patients [1, 30]. Patients with IPMN and NET had similar percentages of PanIN. The association between IPMN and PanIN has been previously described and was confirmed in our series [1, 8, 25]. On the contrary, the association between pancreatic NET and PanIN identified in our study has not been previously described.

We chose to include IPMN, which could be a subject of debate because the ductal abnormalities associated with IPMN, including small ducts, could be misinterpreted as non-communicating PanIN microcysts [1, 7, 30]. However, the results of our pathological correlation show that the small non-communicating cysts we saw were related to PanIN but not BD-IPMN.

There are several limitations to our study including its retrospective design with a potential inclusion bias. However, we tried to avoid most biases by only including patients without or with moderate main pancreatic duct dilatation. Second, one of our main imaging features was non-communicating cyst on MRI and its possible association with PanIN. It does not mean that communication does not exist at pathology. We chose this criterion to avoid possible false-positive cases on IPMN. Third, the presence of PanIN was assessed by histopathological analysis of the resected pancreas, which could underestimate the prevalence of PanIN. Nevertheless, this is the first radiopathological study of PanIN in a large patient cohort. Finally, assessment was focused on identifying possible imaging features associated with PanIN. This could increase the rate of detection of tiny cysts because readers were probably more attentive to small cysts because this was the feature they were asked to report. However, the control group was

Table 4 Results of univariate and multivariate analyses using a conditional logistic regression model for several variables found in a series of 65 patients with PanIN and 35 patients without PanIN

Univariate analysis		Multivariate analysis		
Effect	OR [95%CI]	*p* value	OR [95%CI]	*p**
Microcysts 1 vs. 0	3.7 [1.4–9.35]	0.0044	3.371 [1.297–8.764]	0.0127
Global atrophy 1 vs. 0	11.1 [1.4–87.7]	0.0049	9.787 [1.21–79.129]	0.0324
Focal atrophy 1 vs. 0	0.33 [0.053–2.13]	0.34		
HypoT1 1 vs. 0	1.5 [0.487–4.62]	0.47		
Global atrophy and microcysts 1 vs. 0	Infinity [1.31–infinity]	0.0134		
Global atrophy or microcysts 1 vs. 0	4.622 [1.86–11.45]	0.0006		
No atrophy nor microcysts 1 vs. 0	0.216 [0.08–0.53]	0.0006		

OR, odds ratio; *95%CI*, 95% exact confidence interval. 1 vs. 0 means present vs. absent. *Indicates exact conditional logistic regression. Odd ratios and 95%CI are not shown for some variables because zero value in the corresponding cell frequencies (Table 3) led to unstable estimate of these parameters

Table 5 Sensitivity, specificity, and accuracy are estimated with their corresponding 95% confidence intervals (CI) for categorical variables found in a series of 65 patients with PanIN and 35 patients without PanIN

Variable	TP	FP	FN	TN	n	Se (Pr) [95%CI]	Sp (Pr) [95%CI]	Ac (Pr) [95%CI]
Microcysts	34	8	31	27	100	52.31 (34/65) [51.92–52.70]	77.14 (27/35) [76.70–77.59]	61 (61/100) [50.7–70.6]
Global atrophy	16	1	49	34	100	24.62 (16/65) [24.28–24.95]	97.14 (34/35) [96.97–97.32]	50 (50/100) [39.83–60.17]
Focal atrophy	1	2	64	33	100	1.54 (1/65) [1.44–1.63]	94.6 (33/35) [94.36–94.83]	34 (34/100) [24.82–44.15]
Focal hypoT1W	12	3	53	32	100	18.46 (12/65) [18.16–18.76]	92.11 (33/35) [91.83–02.38]	44 (44/100) [34.08 54.28]
Global atrophy and microcysts	10	0	55	35	100	15.39 (10/65) [15.10–15.67]	100 (0/35) [0.7225–1]	45 (45/100) [35.03–55.27]
Global atrophy or microcysts	30	9	35	26	100	46.15 (30/65) [45.77–46.54]	74.29 (26/35) [73.82–74.75]	56 (56/100) [45.72–65.92]
No atrophy nor microcysts	25	26	40	9	100	38.46 (25/65) [38.08–38.84]	25.71 (9/35) [25.25–26.18]	31 (31/100) [22.13–41.03]

Numbers in parentheses are proportions. Numbers in brackets are 95% exact confidence interval. *TP*, true positive; *FP*, false positive; *FN*, false negative; *n*, number; *TN*, true negative; *Se*, sensitivity; *Sp*, specificity; *Ac*, accuracy; *95%CI*, 95% exact confidence interval; *Pr*, proportions; *T1W*, 1-weighted MR image

included to assess the diagnostic value of our results. Moreover, interobserver variability was excellent for the presence of non-communicating microcysts on MR imaging, confirming the reliability of our findings. Indeed, we acknowledge that our surgical population might be different from a general population and our results cannot be extrapolated.

In conclusion, our study shows a significant association between the presence of non-communicating microcysts on MR imaging and the presence of PanIN on histopathological analysis in patients with tumors and pancreatectomy. In patients enrolled in screening programs, these imaging features should be described. Further prospective and follow-up studies are needed to confirm whether MR imaging can help identify PanIN, in particular, PanIN-3.

Acknowledgments We would like to thank Dale Roche who performed the language editing of this paper.

Funding The authors state that this work has not received any funding.

Compliance with ethical standards

Guarantor The scientific guarantor of this publication is Dr. Marie-Pierre Vullierme MD.

Conflict of interest The authors of this manuscript declare no relationships with any companies, whose products or services may be related to the subject matter of the article.

Statistics and biometry Dr. Tony Ibrahim and Pr Vinciane Rebours kindly provided statistical advice for this manuscript.

Both authors have significant statistical expertise.

No complex statistical methods were necessary for this paper.

Informed consent Written informed consent was not required for this study because the study was retrospective upon preoperative MRI.

Written informed consent was waived by the Institutional Review Board.

Ethical approval Institutional Review Board approval was obtained.

Methodology
- retrospective
- case-control study
- performed at one institution

References

1. Matsuda Y, Furukawa T, Yachida S et al (2017) The prevalence and clinicopathological characteristics of high-grade pancreatic intraepithelial neoplasia (PanIN) – autopsy study evaluating the entire pancreatic parenchyma. Pancreas 46(5):658–664
2. Klöppel G, Lüttges J (2001) WHO-classification 2000: exocrine pancreatic tumors. Verh Dtsch Ges Pathol 85:219–228
3. Hruban RH, Takaori K, Klimstra DS et al (2004) An illustrated consensus on the classification of pancreatic intraepithelial neoplasia and intraductal papillary mucinous neoplasms. Am J Surg Pathol 28:977–987
4. Hruban RH, Maitra A, Goggins M (2008) Update on pancreatic intraepithelial neoplasia. Int J Clin Exp Pathol 1(4):306–316
5. Basturk O, Hong SM, Wood LD et al (2015) A revised classification system and recommendations from the Baltimore consensus meeting for neoplastic precursor lesions in the pancreas. Am J Surg Pathol 39(12):1730–1741
6. Murphy SJ, Hart SN, Lima JF et al (2013) Genetic alterations associated with progression from pancreatic intraepithelial neoplasia to invasive pancreatic tumor. Gastroenterology 145(5):1098–1109

7. Distler M, Aust D, Weitz J, Pilarsky C, Grützmann R (2014) Precursor lesions for sporadic pancreatic cancer: PanIN, IPMN, and MCN. Biomed Res Int:474905
8. Maire F, Couvelard A, Palazzo L et al (2013) Pancreatic intraepithelial neoplasia in patients with intraductal papillary mucinous neoplasms: the interest of endoscopic ultrasonography. Pancreas 42(8):1262–1266
9. Brune K, Abe T, Canto M et al (2006) Multifocal neoplastic precursor lesions associated with lobular atrophy of the pancreas in patients having a strong family history of pancreatic cancer. Am J Surg Pathol 30(9):1067–1076
10. Ito H, Kawaguchi Y, Kawashima Y, et al (2015) A case of pancreatic intraepithelial neoplasia that was difficult to diagnose preoperatively. Case Rep Oncol;22 8(1): 30–36
11. Detlefsen S, Sipos B, Feyerabend B, Klöppel G (2005) Pancreatic fibrosis associated with age and ductal papillary hyperplasia. Virchows Arch 447(5):800–805
12. Tirkes T, Shah ZK, Takahashi N et al (2018) Reporting standards for chronic pancreatitis by using CT, MRI, and MR cholangiopancreatography: the consortium for the study of chronic pancreatitis, diabetes, and pancreatic cancer. Radiology 00:1–10
13. Canto MI, Harinck F, Hruban RH et al (2013) International cancer of the Pancreas Screening (CAPS) Consortium summit on the management of patients with increased risk for familial pancreatic cancer. Gut 62:339–347
14. Canto MI, Goggins M, Hruban RH et al (2006) Screening for early pancreatic neoplasia in high-risk individuals: a prospective controlled study. Clin Gastroenterol Hepatol 4(6):766–781
15. Canto MI, Hruban RH, Fishman EK et al (2012) Comparison of CT, MRI, and EUS for detection of prevalent pancreatic lesions (per patient analysis) frequent detection of pancreatic lesions in asymptomatic high-risk individuals screening for early pancreatic neoplasia (CAPS 3 study). Gastroenterology 142(4):796–704
16. Brand RE, Lerch MM, Rubinstein WS et al (2007) Advances in counselling and surveillance of patients at risk for pancreatic cancer. Participants of the fourth international symposium of inherited diseases of the pancreas. Gut 56(10):1460–1469
17. Notta F, Chan-Seng-Yue M, Lemire M et al (2016) A renewed model of pancreatic cancer evolution based on genomic rearrangement patterns. Nature 538(7625):378–382
18. Peters MLB, Eckel A, Mueller PP et al (2018) Progression to pancreatic ductal adenocarcinoma from pancreatic intraepithelial neoplasia: results of a simulation model. Pancreatology:1–7
19. Paroder V, Flusberg M, Kobi M, Rozenblit AM, Chernyak V (2016) Pancreatic cysts: what imaging characteristics are associated with development of pancreatic ductal adenocarcinoma? Eur J Radiol 85:1622–1626
20. Bartsch DK, Dietzel K, Bargello M et al (2013) Multiple small "imaging" branch-duct type intraductal papillary mucinous neoplasms (IPMNs) in familial pancreatic cancer: indicator for concomitant high grade pancreatic intraepithelial neoplasia? Fam Cancer 12(1):89–96
21. Munigala S, Gelrud A, Agarwal B (2016) Risk of pancreatic cancer in patients with pancreatic cyst. Gastrointest Endosc 84(1):81–86
22. Waters JA, Schmidt CM, Pinchot JW et al (2008) CT vs MRCP: optimal classification of IPMN type and extent. J Gastrointest Surg 12(1):101–109
23. Choi JY, Lee JM, Lee MW et al (2009) Magnetic resonance pancreatography: comparison of two- and three-dimensional sequences for assessment of intraductal papillary mucinous neoplasm of the pancreas. Eur Radiol 19(9):2163–2170
24. Harinck F, Konings IC, Kluijt I et al (2015) A multicentre comparative prospective blinded analysis of EUS and MRI for screening of pancreatic cancer in high-risk individuals. Gut 65:1505–1513
25. LeBlanc JK, Chen JH, Al-Haddad M et al (2014) Can endoscopic ultrasound predict pancreatic intraepithelial neoplasia lesions in chronic pancreatitis? A retrospective study of pathologic correlation. Pancreas 43(6):849–854
26. Tanaka M, Fernandez-del Castillo C, Adsay V et al (2012) International consensus guidelines 2012 for management of intraductal papillary mucinous neoplasms and mucinous cystic neoplasms of the pancreas. Pancreatology (12):183–197
27. Balci C (2011) MRI assessment of chronic pancreatitis. Diagn Interv Radiol 17:249–254
28. Frøkjær JB, Olesen SS, Drewes AM (2013) Fibrosis, atrophy, and ductal pathology in chronic pancreatitis are associated with pancreatic function but independent of symptoms. Pancreas 42(7):1182–1187
29. Landis JR, Koch GG (1977) The measurement of observer agreement for categorical data. Biometrics 33(1):159–174
30. Recavarren C, Labow DM, Liang J et al (2011) Histologic characteristics of pancreatic intraepithelial neoplasia associated with different pancreatic lesions. Hum Pathol 42(1):18–24
31. Canto MI, Goggins M, Yeo CJ et al (2004) Screening for pancreatic neoplasia in high-risk individuals: an EUS-based approach. Clin Gastroenterol Hepatol 2(7):606–621